

The near-infrared size-luminosity relations for Herbig Ae/Be disks

J. D. Monnier¹, R. Millan-Gabet², R. Billmeier¹, R. L. Akeson², D. Wallace³, J.-P. Berger⁴, N. Calvet⁵, P. D'Alessio⁶, W. C. Danchi³, L. Hartmann⁵, L. A. Hillenbrand⁷, M. Kuchner⁸, J. Rajagopal³, W. A. Traub⁵, P. G. Tuthill⁹, A. Boden², A. Booth¹⁰, M. Colavita¹⁰, J. Gathright¹¹, M. Hrynevych¹¹, D. Le Mignant¹¹, R. Ligon¹⁰, C. Neyman¹¹, M. Swain¹⁰, R. Thompson², G. Vasisht¹⁰, P. Wizinowich¹¹, C. Beichman², J. Beletic¹¹, M. Creech-Eakman¹⁰, C. Koresko², A. Sargent², M. Shao¹⁰, & G. van Belle²

ABSTRACT

We report the results of a sensitive K-band survey of Herbig Ae/Be disk sizes using the 85-m baseline Keck Interferometer. Targets were chosen to span the maximum range of stellar properties to probe the disk size dependence on luminosity and effective temperature. For most targets, the measured near-infrared sizes (ranging from 0.2 to 4 AU) support a simple disk model possessing a central optically-thin (dust-free) cavity, ringed by hot dust emitting at the expected sublimation temperatures ($T_s \sim 1000\text{-}1500\text{K}$). Furthermore, we find a tight correlation of disk size with source luminosity $R \propto L^{\frac{1}{2}}$ for Ae and late Be systems (valid over more than 2 decades in luminosity), confirming earlier suggestions

¹monnier@umich.edu: University of Michigan Astronomy Department, 941 Dennison Bldg, Ann Arbor, MI 48109-1090, USA.

²Michelson Science Center, California Institute of Technology, 770 South Wilson Avenue, Pasadena, CA 91125

³NASA Goddard Space Flight Center

⁴Laboratoire d'Astrophysique de Grenoble, 414 Rue de la Piscine 38400 Saint Martin d'Heres, France

⁵Harvard-Smithsonian Center for Astrophysics, 60 Garden St, Cambridge, MA, 02138, USA

⁶Universidad Nacional Autónoma de México

⁷Astronomy Department, California Institute of Technology, Pasadena, CA

⁸Princeton University, Princeton, NJ

⁹University of Sydney, Physics Department

¹⁰Jet Propulsion Laboratory, California Institute of Technology, 4800 Oak Grove Drive, Pasadena, CA 91109

¹¹W. M. Keck Observatory, California Association for Research in Astronomy, 65-1120 Mamalahoa Highway, Kamuela, HI 96743

based on lower-quality data. Interestingly, the inferred dust-free inner cavities of the highest luminosity sources (Herbig B0-B3 stars) are *under-sized* compared to predictions of the “optically-thin cavity” model, likely due to optically-thick gas within the inner AU.

Subject headings: accretion disks — radiative transfer — instrumentation: interferometers — circumstellar matter — stars: pre-main sequence — stars: formation

1. Introduction

Young stellar objects (YSOs) are often observed to be surrounded by an optically-thick accretion disk, presumably left-over from early stages of star formation. These disks are expected to evolve into optically-thin “debris” disks as the circumstellar material either accretes onto the central star, is blown out of the system, or coagulates into planetessimals. The disappearance of the optically-thick protostellar accretion disk thus marks a transition between the final stages of star formation and the onset of planet formation. High angular resolution studies of these transition disks effectively test our physical models of accretion as well as reveal the initial conditions for planet-building. In particular, infrared interferometers directly probe the temperature and density structure of gas and dust within the inner AU of YSO disks, critical ingredients in any recipe for planet formation.

Millan-Gabet et al. (1999) first discovered the marked discrepancy between theoretical predictions and the observed near-infrared (NIR) sizes of Herbig Ae/Be stars using the Infrared-Optical Telescope Array (IOTA) Interferometer – the AB Aur disk was found to be many times larger than expected.¹² This pattern has been confirmed again and again, with “large” disk sizes for Herbig Ae/Be stars being found by Keck aperture masking (Tuthill et al. 2001; Danchi et al. 2001), additional IOTA work (Millan-Gabet et al. 2001a), and Palomar Testbed Interferometer observations (Akeson et al. 2000, 2002; Eisner et al. 2003, 2004). More recently, a similar pattern has been found for bright T Tauri disks too (Akeson et al. 2005, 2000; Colavita et al. 2003).

Popular disk theories of that time (e.g., Lynden-Bell & Pringle 1974; Adams et al. 1987; Calvet et al. 1991; Hillenbrand et al. 1992; Hartmann et al. 1993; Chiang & Goldreich 1997) incorporated an optically-thick, geometrically-thin disk (with flaring, which is not so relevant

¹²In this paper, the “disk size” generally refers to the extent of the disk emission at a particular wavelength, not the *physical* extent of all the disk material.

for NIR wavelengths). In these models, the optically-thick disk midplane shields inner dust from much of the stellar radiation, thus hot dust near sublimation temperature ($T_s \sim 1500K$) can exist quite close to the star. Interferometer measurements showed this emission to be much further from the stars than these models predicted, thus arose the size controversy. About the same time, Natta et al. (2001) revisited the problem of the unrealistically high accretion rates inferred for some Herbig Ae/Be stars (based on NIR excess; Hillenbrand et al. 1992; Hartmann et al. 1993) using spectroscopic observations from the Infrared Space Observatory (ISO). These two observational “problems” would be resolved by the same solution.

First suggested by Tuthill et al. (2001) and independently developed by Natta et al. (2001) and Dullemond et al. (2001), the large disk sizes and excess NIR flux were naturally explained by the presence of an *optically-thin* cavity surrounding the star. Thus, the innermost disk is *not* optically thick, presumably because dust, which is the primary source of opacity for $T \lesssim 1500K$, is absent due to evaporation by the stellar radiation field. This geometry explains the NIR excess flux as well since a frontally-illuminated dust wall efficiently emits in the NIR. Interestingly, earlier modellers had already realized the inner cavity would be devoid of dust due to the high temperatures (e.g., Hillenbrand et al. 1992), but the temperature profile adopted by these workers still implicitly incorporated an optically-thick disk midplane. These central cavities are not necessarily devoid of gas; indeed, the optical depth of the gas depends on many factors (most notably, the accretion rate and geometry). Central clearings in YSO disks are not only interesting in the context of accretion disk physics but have been implicated in halting migration of the extrasolar hot Jupiter planets (Kuchner & Lecar 2002).

Monnier & Millan-Gabet (2002) put the “optically-thin cavity” model to the most stringent test thus far by analyzing the full set of published interferometer measurements (including both T Tauri and Herbig Ae/Be stars for the first time) and found overall consistency through the use of a “size-luminosity” diagram. This diagram is particularly powerful because the inner radius of dust destruction is nearly independent of stellar temperature and almost a pure function of luminosity. This work also uncovered evidence for possible absorption by the *gaseous* inner disk of the most luminous sources in the sample, although interpretation was limited by significant data scatter due (at least in part) to the heterogeneous nature of the datasets.

Recently, Eisner et al. (2003, 2004) made significant contributions to the studies of these disks in a number of ways. Firstly, they measured elongated NIR emission from some Herbigs, evidence for disk-like structure that had eluded the shorter-baseline IOTA work. Furthermore, the size-luminosity relations of Monnier & Millan-Gabet (2002) were confirmed

for the Herbig Ae stars. Perhaps most interestingly, Eisner et al. (2004) presented the clearest evidence to-date for *under-sized* disk emission around the early B stars in their sample. In fact, the NIR sizes of these disks were found consistent with the “classical” optically-thick, geometrically-thin disk models.

Within this context, our group has carried out a survey of YSOs as part of “shared-risk” commissioning of the Keck Interferometer. The Keck Interferometer boasts 10–100× the sensitivity over previous-generation instruments, allowing a large number of Herbig Ae/Be, T Tauris, and FU Orionis objects to be targeted. In order to extend beyond existing work, we designed our survey as follows. First, great care was taken to choose targets with reliable spectral types and luminosities (early interferometers could detect relatively few targets and many had ambiguous classifications). Second, the greater instrumental sensitivity allowed us to probe systems spanning a larger range of spectral types and stellar luminosities.

Here we report our results for the Herbig Ae/Be portion of the survey, where we have significantly reduced the observational “scatter” that hampered previous studies. With the improved data quality, we can definitively characterize the size-luminosity relations of Herbig Ae/Be disks.

2. Observations

The Keck Interferometer (KI) was used during its visibility science commissioning period (2002-2004) to observe 14 Herbig Ae/Be stars as part of this survey (see Table 1). The KI is formed by two 10-m aperture telescopes (each consisting of 36 hexagonal mirror segments) separated by 85 m along a direction \sim 38 degrees East of North, corresponding to a minimum fringe spacing of 5.3 milli-arcseconds at $2.2\mu\text{m}$. In order to coherently combine the NIR light from such large apertures, each telescope utilizes a natural guide star adaptive optics system (Wizinowich et al. 2003). Optical delay lines correct for sidereal motion and the telescope beams are combined at a beamsplitter before the light is focused onto single-mode (fluoride) fibers which impose a \sim 50 milliarcsecond (FWHM) field-of-view for all data reported herein. While both H and K-band observations are now possible, only broad K-band ($2.18\mu\text{m}$, $\Delta\lambda = 0.3\mu\text{m}$) data are reported here. Owing to the large apertures and excellent site, the Keck Interferometer is currently the world’s most sensitive infrared interferometer, recently becoming the first such instrument to measure fringes on an extra-galactic object (Swain et al. 2003). Further technical details can be found in recent Keck Interferometer publications (Colavita et al. 2003; Colavita & Wizinowich 2003, 2000).

Table 1 summarizes the basic properties of the target stars, including spectral type,

distance, luminosity, and literature references for photometry used herein. Calibration of fringe data was performed by interspersing target observations with those of unresolved calibrators (see Table 2). The square of the fringe visibility (V^2) was measured using the ABCD-method (using a dither mirror; see also Shao & Staelin 1977) and we followed the well-tested strategies described for the Palomar Testbed Interferometer (Colavita 1999), except that corrections for uneven telescope ratios were improved and jitter corrections were not applied. We refer the reader to Colavita et al. (2003) and Swain et al. (2003) for further description of calibration procedures.

The calibrated V^2 results appear in Table 3 along with with the projected baseline (u,v) and date for each independent dataset. The V^2 errors reported in this table only include statistical errors. Internal data quality checks have established a conservative upper limit to the systematic error $\Delta V^2 = 0.05$. Model fitting in this paper includes both sources of error in the uncertainty analysis.

3. Methodology

In this study, we wish to measure the characteristic NIR sizes of YSO accretion disks. By using a target sample spanning a wide range of stellar properties, we aim also investigate the size dependence on stellar luminosity. Interferometers have been successfully used to resolve stars since 1921 (Michelson & Pease 1921), and a full discussion of the methodology will not be given here. A single-baseline interferometer can effectively determine the characteristic size of an astronomical object by measuring the fringe “visibility,” a measure of the fringe contrast; unresolved sources produce high contrast fringes (visibility unity) while resolved objects have low visibility (for further discussion, see Thompson et al. 2001). Visibility data can be converted into a quantitative “size” estimate by using a model for the brightness distribution and applying a Fourier Transform. Since we can not *image* the disks directly yet, we must adopt a simple empirical model capable of parameterizing the spatial extent of the disk emission.

Monnier & Millan-Gabet (2002) discuss the merits of using a “ring” model for describing the NIR emission from a circumstellar disk, based on the argument that only the hottest dust at the inner edge of the disk can contribute significantly to the NIR emission (see also Natta et al. 2001). Ring models have been fit to visibility data by other workers in the field as well (Millan-Gabet et al. 2001b; Eisner et al. 2003, 2004). Furthermore, the first imaging results for the LkH α 101 disk (Tuthill et al. 2001) appear to support this class of models.

We have fitted our visibility data with a simple model consisting of a point source (rep-

resenting the unresolved stellar component) and a thin (circular) ring with average diameter θ (representing the circumstellar dust emission). The thickness of the ring can not be easily constrained for measurements on the main lobe of the visibility curve (i.e, when the fringe spacing is less than the ring diameter) and thus our results are only sensitive to the *average* ring diameter, not the ring thickness. For the fits reported here, we have used a uniform brightness ring with a fractional thickness of 20%, inspired by the LkH α 101 image.

Because our interferometer measurements lack the requisite (u,v) coverage to fully constrain our ring model, the fraction of the total K-band emission coming from the disk must be estimated separately through SED fitting. This method was first applied to interferometry observations of YSOs by Millan-Gabet et al. (1999) and is now in common usage (Millan-Gabet et al. 2001a; Akeson et al. 2000, 2002; Eisner et al. 2003, 2004). Here, we fit the broadband SED with a two-component model, consisting of a stellar spectrum and a single-temperature dust blackbody. We have slightly improved on the standard procedure by using a Kurucz model (Kurucz 1979) for the underlying stellar spectrum instead of a simple blackbody, which makes some difference for sources with small IR excess or cool stellar atmospheres. Reddening of the central star must also be included in the fit, and here we adopted the reddening law from Mathis (1990); this choice affects our (de-reddened) luminosity estimates for the most obscured targets.

Figure 1a shows an example of our spectral decomposition for the A8V target HD 142666; the two-component fit is quite acceptable. From the fitting results, only two parameters are used in subsequent analysis: the K-band IR excess and the star luminosity (in cases where good literature estimates are unavailable; see Table 1). In particular, the best-fit dust temperature and flux are not directly used in visibility fitting since the ring model is purely *geometric*. We note that scattered stellar light can not be distinguished from direct stellar emission in the SED, thus the point source component might be somewhat underestimated; this effect is minimized by observing at K band, where scattering is much less efficient than for J or H bands.

Because YSOs are often variable sources, we were concerned with making reliable estimates of the K-band IR excess based on non-contemporaneous photometry. We have adopted the following procedure to conservatively estimate our observational uncertainties. We created multiple synthetic SEDs using various combinations of visible (typically, B,V,R) and infrared photometric datasets drawn from the literature. For each SED we obtained an estimate of the fraction of light at K-band arising from the circumstellar dust through model-fitting. The fitting results for the IR excess naturally depended on the exact photometry data used, and this variation was quantified (typically $\sim 10\%$) and reported in Table 4 for all targets. The “best estimate” was based on the SED with the most recent IR photometry

(usually from 2MASS).

Once the NIR excess has been separately estimated, a ring model can be fit to the KI visibility data with only one free parameter, the ring diameter (having already adopted a 20% ring thickness). This process is illustrated for HD 142666 in Figure 1b, showing fitting results for 3 different estimates of the fraction of K-band emission coming from the dust component (“dust fraction”). Table 4 contains the complete fitting results for all sources, listing the ring diameters along with errors including both the visibility measurement error and our uncertainty in dust fraction. The reported uncertainty in the ring diameter is often dominated by our uncertainty in estimating the dust fraction, instead of V^2 measurement errors.

With our current single-baseline observations, we are unable to detect disk elongations if present, such as those reported by Eisner et al. (2003, 2004). Based on these workers’ data, we can expect up to a 50% variation in ring diameter depending on the orientation of the disk on the sky, and this source of scatter will be discussed further in §4.1.

4. Results

The results of our model fits can be found in Table 4. All but one source were resolved by the Keck Interferometer (the transition object HD 141569 was unresolved), and the ring diameters ranged from \sim 1.5 mas to 4 mas. In order to compare the ring diameters of different sources, we have converted angular diameters (milliarcseconds) into physical sizes (AU) using the estimated distances (drawn from the literature), and these values are also tabulated.

A few of our survey targets (MWC 758, HD 141569, v1685 Cyg, v1977 Cyg) were observed recently by Eisner et al. (2004) using the Palomar Testbed Interferometer (PTI). Comparing average ring diameter results, we find that PTI and KI results agree at the $1-2\sigma$ level. This reasonable agreement suggests that neither experiment is contaminated with large-scale scattered light, since the PTI experiment has a $20\times$ larger field-of-view than the KI observations. While agreement between these two datasets is generally satisfactory, we note an apparent inconsistency between the PTI and KI data for v1685 Cyg along one particular position angle. The current PTI data has a relatively low signal-to-noise ratio, making a definitive comparison uncertain; future work will investigate this apparent discrepancy in more detail.

4.1. Size-Luminosity Diagram

In order to investigate specific accretion disk models, we wish to compare the observed physical sizes of the NIR emission to model predictions. Since the NIR emission should be dominated by hot dust at the inner edge of the dusty disk, we expect the truncation radius to be some function of the stellar luminosity. Thus, we have plotted our results on a size-luminosity diagram (Figure 2) using the parameters compiled in Table 1, as first described in Monnier & Millan-Gabet (2002). Since we have used a ring model for our emission geometry, the ring radius (which we measured by fitting to the visibility data) can be identified with the dust destruction radius, the location where the dust temperature exceeds the sublimation temperature.

In Figure 2, we compare our observational results to predictions of a simple physical model for the dusty circumstellar environment. Here, we assume the star is surrounded by an optically-thin cavity and that dust is distributed in a disk geometry at larger radii. The size of the inner cavity is set by the dust sublimation radii R_s (for sublimation temperature T_s) and can be calculated from basic radiation transfer (see Figure 3a for schematic drawing). In this model, spherical dust grains at the inner edge are in thermal equilibrium with the unobscured central star of luminosity L_* , leading to a standard result (Monnier & Millan-Gabet 2002):

$$R_s = \frac{1}{2} \sqrt{\epsilon_Q} \left(\frac{T_*}{T_s} \right)^2 R_* = 1.1 \sqrt{\epsilon_Q} \left(\frac{L_*}{1000 L_\odot} \right)^{\frac{1}{2}} \left(\frac{T_s}{1500 K} \right)^{-2} AU \quad (1)$$

where $\epsilon_Q = Q_{\text{abs}}(T_*)/Q_{\text{abs}}(T_s)$ the ratio of the dust absorption efficiencies $Q(T)$ for radiation at color temperature T of the incident and reemitted field respectively.

We note that the sublimation radius derived by Dullemond et al. (2001, see Eq. 14) is a factor of 2 times larger than Eq. 1, since these workers assume the dust forms an optically-thick “hot inner wall” at R_s . Recent work by Whitney et al. (2004) found sublimation radii close to that expected in this optically-thick limit. In reality, R_s will be between these limits depending how abruptly the dust becomes optically thick as a function of radius.

Inspection of Figure 2 reveals that Herbig targets between $1 L_\odot < L_* < 10^3 L_\odot$ have ring radii consistent with the calculated dust sublimation radii R_s for sublimation temperatures $T_s \sim 1000\text{-}1500 K$, and the observed sizes are tightly correlated with stellar luminosity. The data points in the Keck Interferometer size-luminosity diagram show much less scatter around the $R \propto L^{\frac{1}{2}}$ trendlines than was seen in previous studies (especially, Monnier & Millan-Gabet 2002). We owe the reduced scatter to the homogeneous nature of our dataset and the improvements in the experimental methodology, including better target vetting for reliable

spectral types, higher angular resolution, use of K band (instead of H band) and smaller field-of-view to reject scattered light, and lastly higher signal-to-noise ratio. These high-quality data offer definitive confirmation of the size-luminosity relations $R \propto L^{\frac{1}{2}}$ for Herbig Ae and late Be disks, strong evidence for the optically-thin cavity model.

The remaining size scatter of about 50% is likely due to inclination effects, consistent with the range of elongations observed by Eisner et al. (2003, 2004). Further evidence for this comes from the fact that UX Ori, which is widely believed to be viewed at high inclination angle (e.g., Natta et al. 1999), is one of the most extreme targets in Figure 2, showing the lowest apparent sublimation temperature. We note that our visible-light sensitivity limit ($R \lesssim 10.5$) introduces a bias against edge-on sources if the disk heavily obscures the star.

We appreciate that the true NIR brightness distribution of YSO disks may not be adequately described by the ring model adopted here, despite our sound scientific motivations. Only future imaging work by IOTA, CHARA, and/or VLTI interferometers will unambiguously establish the true emission geometry. However, regardless of the exact emission morphology, the size-luminosity trends presented here should still remain valid if the targets in our sample share a common emission geometry.

4.2. “Under-sized” disks around high luminosity sources

While the “optically-thin cavity” model can explain the observed sizes of Herbig Ae and late Be stars, the higher luminosity (high-L) sources clearly deviate from the model predictions. These measured disk sizes are many times too small to be consistent with the size-luminosity relations found for the lower luminosity sources. While our sample only contains two such sources, v1685 Cyg (B3) and Z CMa A (B0?), the results must be taken seriously given the unambiguous discrepancy that can not be explained by known sources of uncertainty (however, see §4.3 for specific discussion of the problematic Z CMa system).

In order to investigate this further, we have calculated the dust sublimation radii for an alternate disk model: the “classical” optically-thick, geometrically thin disk model for $T_s \sim 1500\text{ K}$ and 1000 K (e.g., Hillenbrand et al. 1992; Millan-Gabet et al. 2001a). The main difference from the previous model is that a thin disk of gas acts to shield the dusty disk from direct stellar illumination. Thus, the expected sublimation radii R_s are significantly smaller than for the corresponding optically-thin cavity model. Figure 3 contains a sketch contrasting the two model geometries under investigation here.

The dust destruction radius for the classical accretion disk model is not a pure function of luminosity (see above references for derivation of analytical formulation) and thus a separate

model estimate must be made for each target based on specific stellar parameters. The results of this calculation are plotted in Figure 4 along with the Keck Interferometer disk sizes and the previously-derived size-luminosity relations (e.g., Eq. 1). Here we see that the high-L targets are fit better by “classical” accretion disk models than by the optically-thin cavity models, confirming recent analysis of Eisner et al. (2004, based on v1685 Cyg, MWC 1080, and MWC 297).

We can look for further confirmation of this trend by re-considering the results of Monnier & Millan-Gabet (2002). These authors also found many high-L disks to have “undersized” emission, although a few notable targets showed *order-of-magnitude* larger sizes than their high-L peers. Notably, MWC 349 and LkH α 101 (targets resolved by aperture masking) were much larger than their counterparts measured with long-baseline interferometry. Perhaps these sources represent more evolved systems where strong stellar winds have either cleared the inner disk of gas or photo-evaporation has eroded the inner disk. Regardless, our Keck Interferometer results reveal a population of high-luminosity YSOs with disk sizes much smaller than possible for models with optically-thin inner cavities.

In summary, our new Keck Interferometer data support the conclusions of previous studies that some high-luminosity (early Herbig Be) stars show evidence for significant gaseous inner disks. There appears to be a diversity of such disks, from those consistent with *completely* optically-thick disk midplanes (Eisner et al. 2004, and this work) to those with intermediate-tau inner cavities (perhaps optically-thick only in the ultraviolet; see Monnier & Millan-Gabet 2002). We note that dust destruction radii data alone can not directly constrain the geometry of the inner gaseous material – a completely optically-thick midplane has a similar effect to an intermediate-tau spherical gas distribution. In order to distinguish between these scenarios, one must incorporate other observations that also probe the inner accretion disk, such as *mid-infrared* disk sizes (e.g., recently reported by Hinz et al. 2001; Leinert et al. 2004) and high-resolution spectroscopy of the molecular gas (e.g., Najita et al. 2003; Brittain et al. 2003).

4.3. Comments on individual sources

HD 141569: HD 141569, the only unresolved target in our survey, is thought to be in a transition stage between pre-main sequence disk and debris disk. Although disk structures can be seen in scattered light (Clampin et al. 2003), SED modeling by Li et al. (2003) (and others) suggest that nearly all the NIR emission is from the star and that the disk emits significant radiation only at longer wavelengths. Our own SED-fitting and Keck interferometry data support this picture.

UX Ori: UX Ori is the prototype of pre-main sequence objects showing deep visual minima interpreted as obscuration by dust clouds. UXOR behavior is thought to arise for YSOs (typically Herbig Ae/Be stars) which are viewed at high inclination (e.g., Natta et al. 1999), such that our line-of-sight partially intercepts the accretion disk. Under these conditions, we expect the simple “ring” emission geometry (assumed here for visibility fitting) to break down. As we discussed in §4.1, UX Ori has a relatively large disk size, showing a deviation from the mean size-luminosity relations of Figure 2. The NIR emission of UX Ori is likely not ring-like and we may be seeing scattered light if the inner disk emission is partially obscured by the outer flared disk. Clearly, UX Ori is a prime target for interferometric imaging with VLTI and CHARA.

HD 58647: According to Figure 2, this disk is unusually small considering its luminosity. In fact, it has the hottest inferred dust sublimation temperature of the low-luminosity Herbigs. Recently, Manoj et al. (2002) argued that this source is more likely a classical Be star rather than a pre-main-sequence object. Indeed, if the NIR emission is partly arising from free-free (gas) emission, we would expect the observed interferometric size to be small.

Z CMa: This binary source consists of a Herbig (Z CMa A) and an FU Orionis object (Z CMa B) in a close (~ 100 milliarcsecond) orbit (e.g., Garcia et al. 1999; Koresko et al. 1991). The Keck Interferometer was able to observe both sources independently using the 50 milliarcsecond resolution of the adaptive optics system (the FUOR component will be treated in Millan-Gabet et al., in preparation). Determining the photometric contributions of the two components separately is problematic due to strong variability and the small angular separation.

This source is also highly embedded (Hartmann et al. 1989; Whitney et al. 1993) and thus the applicability of the “ring model” for describing the NIR emission is suspect. In addition, the spectral type and luminosity of the Herbig component is highly uncertain – with a factor of 100 in luminosity separating two reasonable estimates. We adopt a lower limit of $3000 L_\odot$ here based on the bolometric luminosity of the system (Hartmann et al. 1989), while an upper limit of $310000 L_\odot$ comes from de-reddening an assumed B0III spectral type (van den Ancker et al. 2004). Obviously this large luminosity uncertainty makes definitive analysis of the Keck Interferometer data impossible, and we encourage follow-up spectroscopic and interferometric observations to confirm the properties of this unique and challenging source.

5. Conclusions

We have definitively measured the near-infrared size-luminosity relations for disks around Herbig Ae/Be stars for $L_* < 10^3 L_\odot$. Valid over more than 2 decades in stellar luminosity L , the NIR sizes obey the simple scaling relation $R \propto L^{\frac{1}{2}}$. This relation is predicted by the “optically-thin cavity” model for YSO disks (Tuthill et al. 2001; Natta et al. 2001; Monnier & Millan-Gabet 2002) and our results imply dust sublimation temperatures in the expected range of $T_s \sim 1000 - 1500 K$.

In contrast, the infrared sizes of circumstellar disks for the high-luminosity sources in our sample ($L_* > 10^3 L_\odot$) are more consistent with *optically-thick* inner disks, supporting recent conclusions of Eisner et al. (2004). Significant gas in the inner disk midplane could explain these observational results, although the gas spatial distribution is not *directly* constrained here. Exceptions to this trend are notable (LkH α 101 and MWC 349, reported elsewhere), perhaps signaling the clearing of the inner gaseous disk by the strong stellar winds and ionizing radiation from evolved O and early B stars.

Future work will progress on two fronts, one theoretical and the other observational. We will focus on using state-of-the-art physical models to fit SEDs and visibilities at both near-IR and mid-IR wavelengths. Such work will allow us to move beyond merely-qualitative tests of new disk models (e.g., the DDN models, Dullemond et al. 2001), for instance by quantifying the optical depth and geometry of the inner gaseous disk. These studies will provide the density and temperature profiles needed for studies of planet formation.

To advance observationally, more single-baseline data are still needed for classical T Tauri disks (Akeson et al., in preparation), FU Orionis stars (Millan-Gabet et al., in preparation), and also for the highest luminosity sources. In contrast, studies of Herbig Ae disks will not be significantly advanced with more single-baseline data, given the (now) large body of existing results; Herbig Ae disks should now be *imaged* to make additional progress. With closure phase imaging from IOTA, VLTI and/or CHARA interferometers, we will test predictions of the next-generation of *physical* models, such as those incorporating a “puffed-up inner wall” (DDN).

The authors wish to thank the all members of the Keck Interferometer development team (JPL, MSC, WMKO) whose dedicated efforts made this “shared-risk” commissioning science possible. This material is based upon work supported by NASA under JPL Contracts 1236050 & 1248252 issued through the Office of Space Science. Data presented herein were obtained at the W.M. Keck Observatory from telescope time allocated to the National Aeronautics and Space Administration through the agency’s scientific partnership with the

California Institute of Technology and the University of California. The Observatory was made possible by the generous financial support of the W.M. Keck Foundation. This research has made use of the SIMBAD database, operated at CDS, Strasbourg, France. This publication makes use of data products from the Two Micron All Sky Survey (2MASS), which is a joint project of the University of Massachusetts and the Infrared Processing and Analysis Center/California Institute of Technology, funded by the National Aeronautics and Space Administration and the National Science Foundation. This work has made use of services produced by the Michelson Science Center at the California Institute of Technology. The authors wish to recognize and acknowledge the very significant cultural role and reverence that the summit of Mauna Kea has always had within the indigenous Hawaiian community. We are most fortunate to have the opportunity to conduct observations from this mountain.

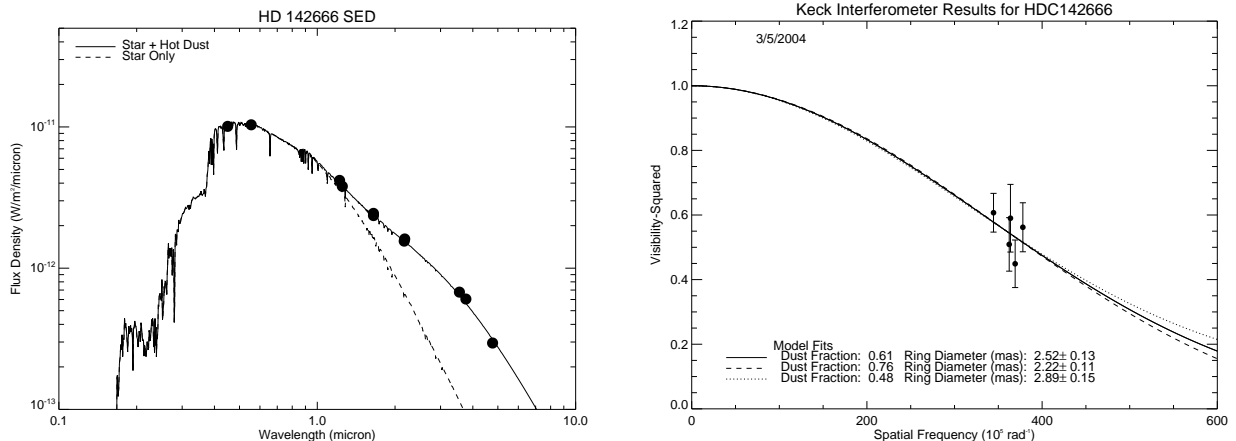


Fig. 1.— a) SED fit for HD 142666, including (reddened) A8V stellar spectrum plus hot dust blackbody ($T = 1355\text{ K}$). Solid points are photometry from the HST Guide Star Catalog (Morrison et al. 2001), 2MASS (Cutri et al. 2003), and the Catalog of Infrared Observations (Gezari et al. 1999). b) Ring model fits to the Keck Interferometer visibility data for three different estimates of the dust fraction at $2.2\mu\text{m}$. The three dust fractions represent the range of possible values derived from the SED fitting process (see §3).

REFERENCES

Adams, F. C., Lada, C. J., & Shu, F. H. 1987, ApJ, 312, 788

Akeson, R. L., Ciardi, D. R., van Belle, G. T., & Creech-Eakman, M. J. 2002, ApJ, 566, 1124

Akeson, R. L., Ciardi, D. R., van Belle, G. T., Creech-Eakman, M. J., & Lada, E. A. 2000, ApJ, 543, 313

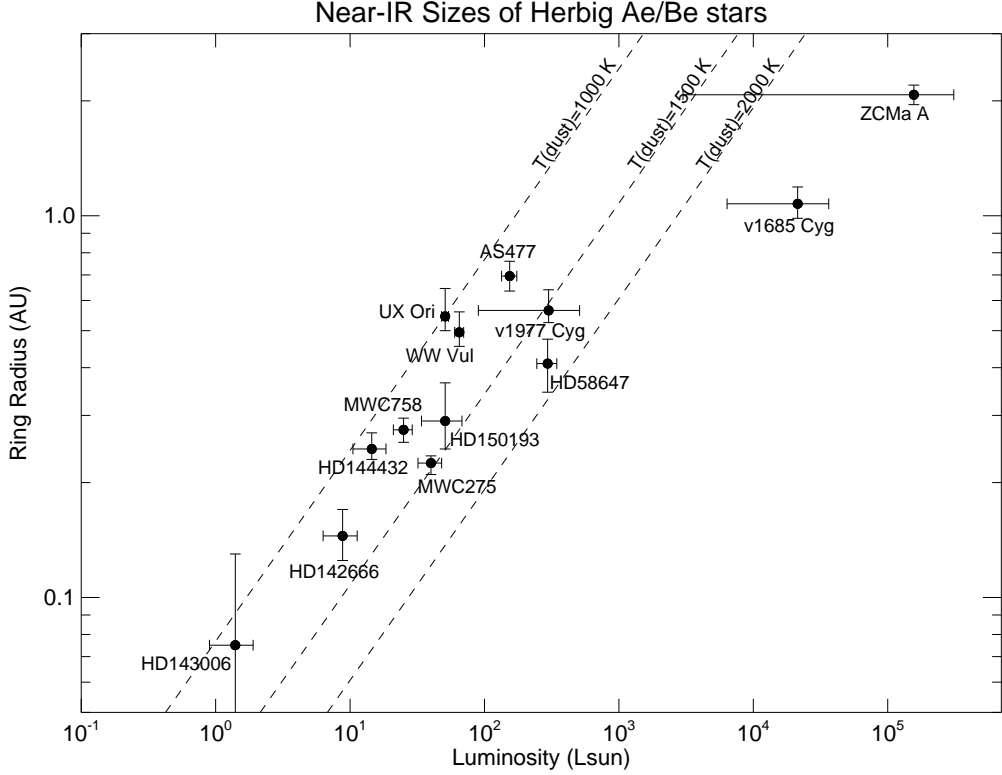


Fig. 2.— Near-infrared sizes of Herbig Ae/Be stars. The Herbig Ae/Be stars observed by the Keck Interferometer have been located on this “size-luminosity diagram.” The plot symbols show the radius of dust emission for the “ring” model discussed in the text. The dashed lines represent the expected inner edge of a dust disk truncated by dust sublimation at temperatures $T_s = 1000$ K, 1500 K, and 2000 K, assuming an optically-thin inner cavity and grey dust.

Akeson, R. L., Walker, C. H., Wood, K., Eisner, J. A., Scire, E., Penprase, B., Ciardi, D. R., van Belle, G. T., Whitney, B., & Bjorkman, J. E. 2005, ApJ, 0, 0

Beskrovnyaya, N. G., Pogodin, M. A., Miroshnichenko, A. S., Thé, P. S., Savanov, I. S., Shakhovskoy, N. M., Rostopchina, A. N., Kozlova, O. V., & Kuratov, K. S. 1999, A&A, 343, 163

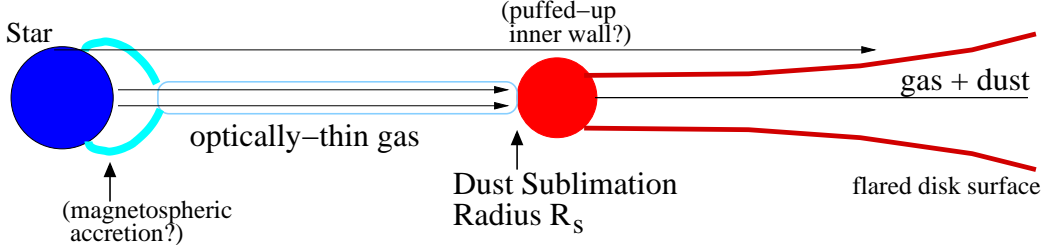
Brittain, S. D., Rettig, T. W., Simon, T., Kulesa, C., DiSanti, M. A., & Dello Russo, N. 2003, ApJ, 588, 535

Calvet, N., Patino, A., Magris, G. C., & D'Alessio, P. 1991, ApJ, 380, 617

Chiang, E. I. & Goldreich, P. 1997, ApJ, 490, 368

Clampin, M., Krist, J. E., Ardila, D. R., Golimowski, D. A., Hartig, G. F., Ford, H. C., Illingworth, G. D., Bartko, F., Benítez, N., Blakeslee, J. P., Bouwens, R. J., Broadhurst, T. J., Brown, R. A., Burrows, C. J., Cheng, E. S., Cross, N. J. G., Feldman,

"Optically-thin Cavity" Disk Model



"Classical" Disk Model

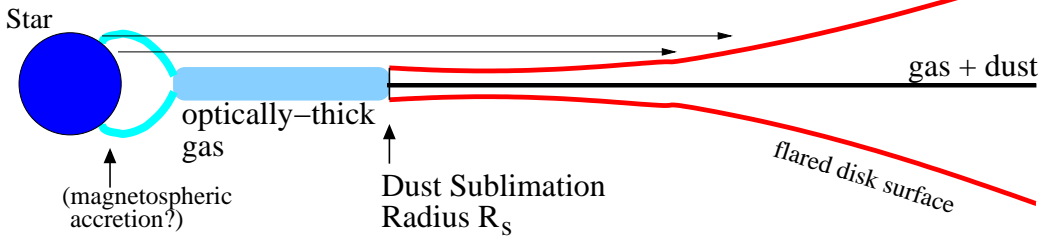


Fig. 3.— Near-infrared sizes of Herbig Ae/Be stars compared to simple models. Here we present schematics of the two disk models under consideration in this paper. (top panel) a. This panel shows a cross-section of the inner disk region for the “optically-thin cavity” model discussed in the text. (bottom panel) b. Here, the cross-section of the “classical” accretion disk model is shown. This model is nearly identical to the first, except the presence of optically-thick gas in the midplane partially shields the innermost dust from stellar radiation, causing the dust sublimation radius (R_s) to shrink for the same sublimation temperature (T_s). In order to place our results in a broader context, we have labelled some additional relevant disk features (magnetospheric accretion columns, disk flaring, puffed-up inner wall) which are not directly constrained by our study.

P. D., Franx, M., Gronwall, C., Infante, L., Kimble, R. A., Lesser, M. P., Martel, A. R., Menanteau, F., Meurer, G. R., Miley, G. K., Postman, M., Rosati, P., Sirianni, M., Sparks, W. B., Tran, H. D., Tsvetanov, Z. I., White, R. L., & Zheng, W. 2003, AJ, 126, 385

Colavita, M., Akeson, R., Wizinowich, P., Shao, M., Acton, S., Beletic, J., Bell, J., Berlin, J., Boden, A., Booth, A., Boutell, R., Chaffee, F., Chan, D., Chock, J., Cohen, R., Crawford, S., Creech-Eakman, M., Eychaner, G., Felizardo, C., Gathright, J., Hardy, G., Henderson, H., Herstein, J., Hess, M., Hovland, E., Hrynevych, M., Johnson, R., Kelley, J., Kendrick, R., Koresko, C., Kurpis, P., Le Mignant, D., Lewis, H., Ligon, E., Lupton, W., McBride, D., Mennesson, B., Millan-Gabet, R., Monnier, J., Moore, J., Nance, C., Neyman, C., Niessner, A., Palmer, D., Reder, L., Rudeen, A., Saloga, T., Sargent, A., Serabyn, E., Smythe, R., Stomski, P., Summers, K., Swain, M.,

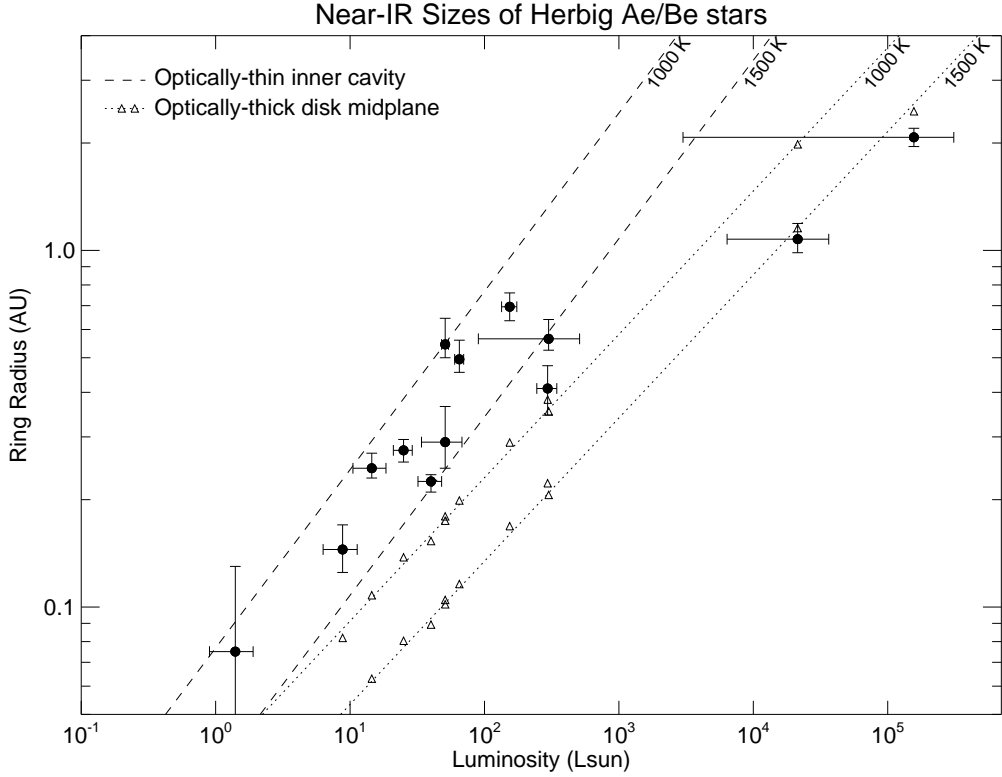


Fig. 4.— The size-luminosity diagram here allows one to compare the observed disk sizes (solid circles) with the predictions of two simple disk models (see Figure 3). The dashed lines show the disk sizes assuming an optically-thin inner disk (same as previous Figure 2), while the dotted lines show mean relations for the inner dust radius predicted for an optically-thick, geometrically-thin inner disk model (open triangles show calculation for individual sources). Both models assume grey dust and results are shown for dust sublimation temperatures $T_s = 1500$ K & 1000 K. Note that if the inner wall of the “optically-thin cavity” model is truly opaque as proposed by Dullemond et al. (2001) then the inferred sublimation temperatures are larger by ~ 500 K (see §4.1 for more discussion).

Swanson, P., Thompson, R., Tsubota, K., Tumminello, A., van Belle, G., Vasisht, G., Vause, J., Walker, J., Wallace, K., & Wehmeier, U. 2003, ApJ, 592, L83

Colavita, M. M. 1999, PASP, 111, 111

Colavita, M. M. & Wizinowich, P. L. 2000, in Proc. SPIE Vol. 4006, p. 310-320, Interferometry in Optical Astronomy, Pierre J. Lena; Andreas Quirrenbach; Eds., 310–320

Colavita, M. M. & Wizinowich, P. L. 2003, in Interferometry for Optical Astronomy II. Edited by Wesley A. Traub. Proceedings of the SPIE, Volume 4838, pp. 79-88 (2003)., 79–88

Cutri, R. M., Skrutskie, M. F., van Dyk, S., Beichman, C. A., Carpenter, J. M., Chester, T.,Cambresy, L., Evans, T., Fowler, J., Gizis, J., Howard, E., Huchra, J., Jarrett, T., Kopan, E. L., Kirkpatrick, J. D., Light, R. M., Marsh, K. A., McCallon, H.,

Schneider, S., Stiening, R., Sykes, M., Weinberg, M., Wheaton, W. A., Wheelock, S., & Zacarias, N. 2003, VizieR Online Data Catalog, 2246, 0

Danchi, W. C., Tuthill, P. G., & Monnier, J. D. 2001, ApJ, 562, 440

Dullemond, C. P., Dominik, C., & Natta, A. 2001, ApJ, 560, 957

Dunkin, S. K., Barlow, M. J., & Ryan, S. G. 1997, MNRAS, 286, 604

Eisner, J. A., Lane, B. F., Akeson, R. L., Hillenbrand, L. A., & Sargent, A. I. 2003, ApJ, 588, 360

Eisner, J. A., Lane, B. F., Hillenbrand, L. A., Akeson, R. L., & Sargent, A. I. 2004, ApJ, 613, 1049

ESA. 1997, VizieR Online Data Catalog, 1239, 0

Friedemann, C., Riemann, H. G., Gurtler, J., & Toth, V. 1993, A&A, 277, 184

Garcia, P. J. V., Thiébaut, E., & Bacon, R. 1999, A&A, 346, 892

Gezari, D. Y., Pitts, P. S., & Schmitz, M. 1999, VizieR Online Data Catalog, 2225, 0

Hartmann, L., Kenyon, S. J., & Calvet, N. 1993, ApJ, 407, 219

Hartmann, L., Kenyon, S. J., Hewett, R., Edwards, S., Strom, K. M., Strom, S. E., & Stauffer, J. R. 1989, ApJ, 338, 1001

Hernández, J., Calvet, N., Briceño, C., Hartmann, L., & Berlind, P. 2004, AJ, 127, 1682

Hillenbrand, L. A., Strom, S. E., Vrba, F. J., & Keene, J. 1992, ApJ, 397, 613

Hinz, P. M., Hoffmann, W. F., & Hora, J. L. 2001, ApJ, 561, L131

Høg, E., Fabricius, C., Makarov, V. V., Urban, S., Corbin, T., Wycoff, G., Bastian, U., Schekendiek, P., & Wicenec, A. 2000, A&A, 355, L27

Joint IRAS Science Working Group. 1988, in IRAS Point Source Catalog (1988), 0–+

Kharchenko, N. V. 2001, Kinematika i Fizika Nebesnykh Tel, 17, 409

Koresko, C. D., Beckwith, S. V. W., Ghez, A. M., Matthews, K., & Neugebauer, G. 1991, AJ, 102, 2073

Kuchner, M. J. & Lecar, M. 2002, ApJ, 574, L87

Kurucz, R. L. 1979, *ApJS*, 40, 1

Lada, C. J. 1985, *ARA&A*, 23, 267

Leinert, C., van Boekel, R., Waters, L. B. F. M., Chesneau, O., Malbet, F., Köhler, R., Jaffe, W., Ratzka, T., Dutrey, A., Preibisch, T., Graser, U., Bakker, E., Chagnon, G., Cotton, W. D., Dominik, C., Dullemond, C. P., Glazeborg-Kluttig, A. W., Glindemann, A., Henning, T., Hofmann, K.-H., de Jong, J., Lenzen, R., Ligori, S., Lopez, B., Meisner, J., Morel, S., Paresce, F., Pel, J.-W., Percheron, I., Perrin, G., Przygoda, F., Richichi, A., Schöller, M., Schuller, P., Stecklum, B., van den Ancker, M. E., von der Lühe, O., & Weigelt, G. 2004, *A&A*, 423, 537

Li, A., Lunine, J. I., & Bendo, G. J. 2003, *ApJ*, 598, L51

Lynden-Bell, D. & Pringle, J. E. 1974, *MNRAS*, 168, 603

Manoj, P., Maheswar, G., & Bhatt, H. C. 2002, *MNRAS*, 334, 419

Mathis, J. S. 1990, *ARA&A*, 28, 37

Meeus, G., Waters, L. B. F. M., Bouwman, J., van den Ancker, M. E., Waelkens, C., & Malfait, K. 2001, *A&A*, 365, 476

Michelson, A. A. & Pease, F. G. 1921, *ApJ*, 53, 249

Millan-Gabet, R. & Monnier, J. D. 2002, *ApJ*, 580, L167

Millan-Gabet, R., Schloerb, F. P., & Traub, W. A. 2001a, *ApJ*, 546, 358

—. 2001b, *ApJ*, 546, 358

Millan-Gabet, R., Schloerb, F. P., Traub, W. A., Malbet, F., Berger, J. P., & Bregman, J. D. 1999, *ApJ*, 513, L131

Monnier, J. D. & Millan-Gabet, R. 2002, *ApJ*, 579, 694

Mora, A., Merín, B., Solano, E., Montesinos, B., de Winter, D., Eiroa, C., Ferlet, R., Grady, C. A., Davies, J. K., Miranda, L. F., Oudmaijer, R. D., Palacios, J., Quirrenbach, A., Harris, A. W., Rauer, H., Cameron, A., Deeg, H. J., Garzón, F., Penny, A., Schneider, J., Tsapras, Y., & Wesselius, P. R. 2001, *A&A*, 378, 116

Morel, M. & Magnenat, P. 1978, *A&AS*, 34, 477

Morrison, J. E., Röser, S., McLean, B., Bucciarelli, B., & Lasker, B. 2001, *AJ*, 121, 1752

Najita, J., Carr, J. S., & Mathieu, R. D. 2003, *ApJ*, 589, 931

Natta, A., Prusti, T., Neri, R., Thi, W. F., Grinin, V. P., & Mannings, V. 1999, *A&A*, 350, 541

Natta, A., Prusti, T., Neri, R., Wooden, D., Grinin, V. P., & Mannings, V. 2001, *A&A*, 371, 186

Pérez, M. R., van den Ancker, M. E., de Winter, D., & Bopp, B. W. 2004, *A&A*, 416, 647

Shao, M. & Staelin, D. H. 1977, *Optical Society of America Journal A*, 67, 81

Swain, M., Vasisht, G., Akeson, R., Monnier, J., Millan-Gabet, R., Serabyn, E., Creech-Eakman, M., van Belle, G., Beletic, J., Beichman, C., Boden, A., Booth, A., Colavita, M., Gathright, J., Hrynevych, M., Koresko, C., Le Mignant, D., Ligon, R., Mennesson, B., Neyman, C., Sargent, A., Shao, M., Thompson, R., Unwin, S., & Wizinowich, P. 2003, *ApJ*, 596, L163

Terranegra, L., Chavarria-K., C., Diaz, S., & Gonzalez-Patino, D. 1994, *A&AS*, 104, 557

Thompson, A. R., Moran, J. M., & Swenson, G. W. 2001, *Interferometry and synthesis in radio astronomy (Interferometry and synthesis in radio astronomy by A. Richard Thompson, James M. Moran, and George W. Swenson, Jr. 2nd ed. New York : Wiley, c2001.xxiii, 692 p. : ill. ; 25 cm. "A Wiley-Interscience publication." Includes bibliographical references and indexes. ISBN : 0471254924)*

Tuthill, P. G., Monnier, J. D., & Danchi, W. C. 2001, *Nature*, 409, 1012

van den Ancker, M. E., Blondel, P. F. C., Tjin A Djie, H. R. E., Grankin, K. N., Ezhkova, O. V., Shevchenko, V. S., Guenther, E., & Acke, B. 2004, *MNRAS*, 349, 1516

van den Ancker, M. E., de Winter, D., & Tjin A Djie, H. R. E. 1998, *A&A*, 330, 145

Whitney, B. A., Clayton, G. C., Schulte-Ladbeck, R. E., Calvet, N., Hartmann, L., & Kenyon, S. J. 1993, *ApJ*, 417, 687

Whitney, B. A., Indebetouw, R., Bjorkman, J. E., & Wood, K. 2004, *ApJ*, 617, 1177

Wizinowich, P. L., Le Mignant, D., Stomski, P. J., Acton, D. S., Contos, A. R., & Neyman, C. R. 2003, in *Adaptive Optical System Technologies II*. Edited by Wizinowich, Peter L.; Bonaccini, Domenico. *Proceedings of the SPIE*, Volume 4839, pp. 9-20 (2003)., 9–20

Table 1. Basic Properties of Targets

Source Names	RA (J2000)	Dec (J2000)	V mag ^a	K mag ^a	Spectral Type	Distance (pc)	Adopted Luminosity (L_{\odot})	Photometry References
UX Ori, HIP 23602	05 04 29.9908	−03 47 14.280	9.6	7.2	A3 (1)	460 (10)	51±3 (1)	10, 15, 16, 17, 18, 19, 20, 21
MWC 758, HD 36112	05 30 27.5296	+25 19 57.083	8.3	5.8	A8V (9)	200 ⁺⁶⁰ _{−40} (4,5)	25±4 (14)	15, 16, 19, 20, 21, 23
Z CMa A ^b , HIP 34042	07 03 43.1619	−11 33 06.209	9.9	3.8	B0III (13)	1050 (13)	3000 – 310000 (13,26)	13, 20, 24, 25
HD 58647, HIP 36068	07 25 56.0989	−14 10 43.551	6.8	5.4	B9IVe (3,4)	280 ⁺⁸⁰ _{−50} (4,5)	295±50 (14)	15, 16, 19, 20, 21
HD 141569, HIP 77542	15 49 57.7489	−03 55 16.360	7.0	6.8	A0Vev (3,6)	99 ⁺⁹ _{−8} (4,5)	18.5±1.0 (14)	15, 16, 18, 19, 20, 21
HD 142666, v1026 Sco	15 56 40.023	−22 01 40.01	8.8	6.1	A8Ve (3,6,7)	116 (7)	8.8±2.5 (14)	15, 16, 18, 19, 20, 21
HD 143006, HIP 78244	15 58 33.4177	−09 00 12.174	8.4	7.1	G5V (6)	94±35 (5)	1.4±0.5 (14)	15, 16, 18, 19, 20, 21
HD 144432, HIP 78943	16 06 57.9575	−27 43 09.806	8.2	5.9	A9IvVev (3)	145 (8)	14.5±4.0	15, 16, 18, 19, 20, 21, 22
HD 150193, MWC 863A	16 40 17.9221	−23 53 45.180	8.9	5.5	A2IVe (3)	150 ⁺⁵⁰ _{−30} (4,5)	51±17 (14)	10, 15, 16, 18, 19, 20, 21, 22
MWC 275, HD 163296	17 56 21.2879	−21 57 21.880	6.9	4.8	A1VepV (3)	122 ⁺¹⁷ _{−13} (4,5)	40±8 (14)	10, 15, 16, 17, 18, 19, 20, 21
WW Vul, HD 344361	19 25 58.750	+21 12 31.28	10.5	7.3	A2IVe (3)	550 (12)	65±5 (1)	15, 16, 17, 18, 19, 20, 21
v1685 Cyg, MWC 340	20 20 28.2473	+41 21 51.586	10.7	5.8	B3 (1)	980 (4)	21400±15000 (1)	10, 15, 16, 17, 18, 19, 20, 21
v1977 Cyg, AS 442	20 47 37.47	+43 47 24.9	10.9	6.6	B8V (3)	700 (11)	300±210 (14)	15, 16, 17, 19, 20, 21
AS 477, v1578 Cyg	21 52 34.0993	+47 13 43.612	10.2	7.2	A0 (1)	900 (2)	154±20 (1)	10, 15, 16, 17, 18, 19, 20, 21

^aMany of the targets are variable stars and these magnitudes (V band from Simbad, and K band from 2MASS) are merely representative.

^bZ CMa is a binary system (Millan-Gabet & Monnier 2002) consisting of an Herbig Component (A) and an FU Orionis star (B). The V and K magnitudes in the table are for the entire system, although our data reduction isolate the contribution from the Herbig component. The spectral type and luminosity for Z CMa A is highly uncertain – see §4.3 for discussion.

Note. — References: (1) Hernández et al. (2004), (2) Lada (1985), (3) Mora et al. (2001), (4) van den Ancker et al. (1998), (5) ESA (1997), (6) Dunkin et al. (1997), (7) Meeus et al. (2001), (8) Pérez et al. (2004), (9) Beskrovnyaya et al. (1999), (10) Hillenbrand et al. (1992), (11) Terranegra et al. (1994), (12) Friedemann et al. (1993), (13) van den Ancker et al. (2004), (14) SED fitting, this work (15) Morrison et al. (2001), (16) Kharchenko (2001), (17) Morel & Magnenat (1978), (18) Gezari et al. (1999), (19) Simbad Astronomical Database, (20) 2MASS; Cutri et al. (2003), (21) Tycho-2; Høg et al. (2000), (22) DENIS Database, 2nd Release, (23) Joint IRAS Science Working Group (1988), (24) Millan-Gabet & Monnier (2002), (25) Koresko et al. (1991), (26) Hartmann et al. (1989)

Table 2. Calibrator Information

Source Name	Calibrator Name	Spectral Type	V mag	K mag	Adopted Uniform Disk ^a Diameter (mas)
UX Ori	HDC33278	G9V	8.6	6.8	0.12±0.2
	HDC36003	K5V	7.7	4.8	0.55±0.1
	HDC26794	K3V	8.8	6.3	0.24±0.1
MWC 758	HDC27777	B8V	5.7	5.9	0.21±0.1
	HDC29645	G0V	6.0	4.6	0.41±0.2
Z CMa A	HDC48286	F7V	7.0	5.7	0.32±0.1
	HDC52919	K5V	8.4	5.5	0.39±0.1
	HDC60491	K2V	8.2	5.9	0.30±0.1
HD 58647	HDC58461	F3V	5.8	4.9	0.39±0.1
	HDC62952	F2V	5.0	4.2	0.39±0.5
HD 141569 & HD 144432	HDC139909	B9.5V	6.9	7.0	0.16±0.1
	HDC147550	B9V	6.2	6.3	0.21±0.1
HD 142666 & HD 150193	HDC144641	G3V	8.0	6.5	0.15±0.1
	HDC134967	A2V	6.1	6.0	0.28±0.1
HD 143006	HD141107	F2V	7.7	6.9	0.17±0.1
	HD149149	G6V	8.6	7.0	0.12±0.1
MWC 275	HDC157546	B8V	6.3	6.5	0.17±0.1
	HDC174596	A3V	6.6	6.5	0.21±0.1
WW Vul	HDC181047	G8V	8.3	6.5	0.19±0.1
	HDC184198	F7V	8.2	6.9	0.14±0.1
v1685 Cyg & v1977 Cyg	HDC199178	G2V	7.2	5.7	0.20±0.2
v1685 Cyg	HIP102667	K2V	8.8	6.6	0.13±0.2
	HDC192985	F5V	5.9	4.8	0.38±0.1
v1977 Cyg	SAO50092	K0V	8.6	6.3	0.30±0.04
	HDC199998	K2III	8.4	5.7	0.40±0.1
AS 477	HDC201456	F8V	7.9	6.6	0.18±0.1
	HIP109034	K4III	9.5	6.2	0.35±0.5
	HDC199178	G2V	7.2	5.7	0.20±0.2

^aAll diameter estimates were made using *getCal*, which is maintained and distributed by the Michelson Science Center (<http://msc.caltech.edu>). The diameters were estimated by fitting the spectral energy distributions with simple blackbody models.

Table 3. Keck Interferometer Visibilities

Source Name	U.T. Date	Projected Baseline U (m)	V (m)	Visibility-Squared $\lambda_0 = 2.18\mu\text{m}$, $\Delta\lambda = 0.3\mu\text{m}$
UX Ori	2004 Jan 07	55.547	64.015	0.483±0.052
		56.336	63.635	0.476±0.042
MWC 758	2002 Oct 24	50.790	67.981	0.360±0.088
		49.974	68.668	0.337±0.039
Z CMa A	2004 Apr 03	28.806	52.420	0.172±0.015
	2004 Apr 05	34.159	53.142	0.186±0.077
HD 58647	2004 Apr 02	30.502	49.851	0.639±0.098
		27.501	49.411	0.734±0.091
HD 141569	2003 Apr 17	55.224	62.474	0.978±0.065
		54.102	62.180	1.056±0.105
HD 142666	2004 Mar 05	56.538	58.909	0.562±0.059
		56.219	56.564	0.445±0.054
		55.784	55.363	0.586±0.092
		55.647	55.064	0.507±0.066
		53.392	51.838	0.604±0.033
HD 143006	2004 Apr 02	40.097	42.871	0.931±0.197
		36.677	41.635	0.863±0.200
HD 144432	2003 Apr 17	54.460	49.100	0.368±0.018
		54.167	48.628	0.380±0.016
HD 150193	2004 Mar 05	54.858	52.468	0.205±0.023
MWC 275	2003 Apr 17	55.592	55.001	0.188±0.010
		54.449	53.157	0.218±0.015
		53.189	51.683	0.218±0.013
		51.713	50.306	0.232±0.015
WW Vul	2003 Aug 09	37.683	74.410	0.642±0.063
		33.914	75.528	0.558±0.059
v1685 Cyg	2002 Jun 27	41.541	72.969	0.397±0.069
		33.288	77.825	0.420±0.108
v1977 Cyg	2002 Oct 24	45.133	69.368	0.636±0.032
		34.998	76.533	0.640±0.041
AS 477	2002 Oct 24	40.923	71.723	0.703±0.025
		35.262	75.529	0.673±0.054

Table 4. Herbig Ae/Be Disk Properties

Source Name	Dust Fraction at K-band ^a	Ring Diameter mas	Ring Diameter AU
UX Ori	0.70 ^{+0.08} _{-0.16}	2.36 ^{+0.43} _{-0.20}	1.09 ^{+0.20} _{-0.09}
MWC 758	0.72 ^{+0.02} _{-0.04}	2.75 ^{+0.22} _{-0.19}	0.55±0.04
Z CMa A	0.975±0.025	3.95±0.24	4.15±0.25
HD 58647	0.54 ^{+0.10} _{-0.04}	2.93±0.45	0.82±0.13
HD 141569	0.05±0.05	<20	<2
HD 142666	0.61 ^{+0.15} _{-0.13}	2.52 ^{+0.41} _{-0.31}	0.29 ^{+0.05} _{-0.04}
HD 143006	0.53 ^{+0.11} _{-0.03}	1.63 ^{+1.12} _{-1.00}	0.15 ^{+0.11} _{-0.09}
HD 144432	0.62 ^{+0.02} _{-0.07}	3.37 ^{+0.32} _{-0.17}	0.49 ^{+0.05} _{-0.03}
HD 150193	0.67 ^{+0.18} _{-0.17}	3.84 ^{+1.03} _{-0.58}	0.58 ^{+0.15} _{-0.09}
MWC 275	0.71 ^{+0.07} _{-0.01}	3.70 ^{+0.14} _{-0.25}	0.45 ^{+0.02} _{-0.03}
WW Vul	0.88 ^{+0.03} _{-0.14}	1.80 ^{+0.24} _{-0.15}	0.99 ^{+0.13} _{-0.08}
v1685 Cyg	0.94 ^{+0.02} _{-0.09}	2.19 ^{+0.23} _{-0.18}	2.15 ^{+0.23} _{-0.18}
v1977 Cyg	0.94 ^{+0.02} _{-0.17}	1.61 ^{+0.22} _{-0.12}	1.13 ^{+0.15} _{-0.08}
AS 477	0.86 ^{+0.03} _{-0.04}	1.55 ^{+0.14} _{-0.13}	1.39 ^{+0.13} _{-0.12}

^aBest estimate for fraction of K-band light coming from circumstellar material based on most recent photometry. Upper and lower limits are based on SED fitting to diverse data sets and represent the range of possible values given historical variability.